Friction **10**(3): 398–410 (2022)
https://doi.org/10.1007/s40544-020-0469-x
ISSN 2223-7690
CN 10-1237/TH
RESEARCH ARTICLE

Regulating the Nb_2C nanosheets with different degrees of oxidation in water lubricated sliding toward an excellent tribological performance

Hao CHENG[1,2], **Wenjie ZHAO**[1,*]

[1] *Key Laboratory of Marine Materials and Related Technologies, Zhejiang Key Laboratory of Marine Materials and Protective Technologies, Ningbo Institute of Materials Technology and Engineering, Chinese Academy of Sciences, Ningbo 315201, China*

[2] *University of Chinese Academy of Sciences, Beijing 100049, China*

Received: 29 July 2020 / Revised: 14 September2020 / Accepted: 29 October 2020

Abstract: Novel two-dimensional (2D) Nb_2C nanosheets were successfully prepared through a simple lultrasonic and magnetic stirring treatment from the original accordion-like powder. To further study their water-lubrication properties and deal with common oxidation problems, Nb_2C nanosheets with different oxidation degrees were prepared and achieved long-term stability in deionized water. Scanning electron microscope (SEM), transmission electron microscope (TEM), scanning probe microscope (SPM), X-ray powder diffraction (XRD), Raman, and X-ray photoelectron spectrometer (XPS) experiments were utilized to characterize the structure, morphology, and dispersion of Nb_2C nanosheets with different degrees of oxidation. The tribological behaviors of Nb_2C with different degrees of oxidation as additives for water lubrication were characterized using a UMT-3 friction testing machine. The wear scars formed on the 316 steel surface were measured using three-dimensional (3D) laser scanning confocal microscopy. The tribological results showed that a moderately oxidized Nb_2C nanosheet, which owned the composition of $Nb_2C/Nb_2O_5/C$, displayed excellent tribological performance, with the friction coefficient (COF) decreasing by 90.3% and a decrease in the wear rate by 73.1% compared with pure water. Combining the TEM and Raman spectra, it was shown that Nb_2O_5 nanoparticles filled in the worn zone, and the layered Nb_2C and C were adsorbed into the surface of the friction pair to form a protective lubricating film. This combined action resulted in an excellent lubricating performance.

Keywords: MXene; Nb_2C nanosheets; oxidation degree; water lubrication; tribology

1 Introduction

In the mechanical or energy industry, friction reduction, and wear resistance have continuously achieved ideal tribological characteristics [1]. Considering that countless losses are caused by friction and wear [2, 3], the most direct and effective method is to add a lubricant between friction pairs to avoid direct contact between them [4]. Water-based lubricants are widely used in the fields of mechanical lubrication, cutting fluids, and hydraulic fluids owing to their excellent cooling and flame retardant properties as well as their higher safety and lower pollution than oil-based lubricants [5–7]. However, traditional pure water lubricants have gradually failed to meet the requirements of particular applications. In view of this, researchers often choose to add nanoadditives to the water lubricating fluid to enhance its tribological

* Corresponding author: Wenjie ZHAO, E-mail: zhaowj@nimte.ac.cn

performance. Furthermore, two-dimensional (2D) layered materials, such as graphene-based materials [8–14], hexagonal boron nitride, and black phosphorus, are the most common additives, and many scholars have conducted extensive studies around them. Ci et al. [15] explored the tribological behaviors from graphene to fluorographene and found that fluorinated reduced graphene oxide nanosheets (F-rGO) with different degrees of fluorination display excellent tribological properties, which is due to the nanosheets with a small size easily entering the contact surface, and the large interlayer spacing makes the sample show a significant shear capability. Wang et al. [16] evaluated the tribological characteristics of black phosphorus nanosheets as water- and oil-based lubricant additives and found that it exhibited an outstanding resistance to extreme pressure and bearing capacity at high loads. This demonstrated that black phosphorus, as a new additive, displayed an excellent lubrication performance. Moreover, MXene is also a novel 2D layered material, but its lubrication performance has rarely been explored.

MXene was first prepared by the Naguib team in 2011 [17]. The parent phase of MXene is a ternary layered metallized ceramic MAX. The MAX phases have the formula $M_{n+1}AX_n$ (n = 1–3), where M is an early transition metal, A is an element traditionally from groups 13–16, and X is carbon or nitrogen [18]. For the MAX phase materials, because the M–X bond strength is greater than the M–A bond, people selectively etched M–A bonds to obtain 2D MXene materials with large specific surface areas, good electrical conductivities, high hydrophilicities, elastic moduli, and high carrier mobilities [19–21].

However, an accordion-like MXene material is too thick to be stably dispersed in an aqueous solution [22], and its large thickness is not conducive to get themselves into the friction pair, and thus it is necessary to further exfoliate it into nanosheets. The most common method to solve this problem is to add an intercalation agent to make the separation between adjacent layers to finally obtain few or even single-layer MXene materials. Thus, MXene materials can be better dispersed in water [23]. However, oxidation is a common problem in a MXene material [24]. In this study, we prepared Nb_2C nanosheets with different degrees of oxidation to explore its influence on the dispersion and structure of Nb_2C, and whether it was beneficial as a water lubricating additive.

Herein, we adopted the MXene material Nb_2C as raw material and the organic base tetrabutylammonium hydroxide (TBAOH) as the intercalation agent, supplemented by simple magnetic stirring, centrifugation, and ultrasound to reduce the number of layers. The microstructure of Nb_2C was then regulated by controlling its degree of oxidation; thus, the original Nb_2C, moderately oxidized Nb_2C and completely oxidized Nb_2C nanosheets were obtained. Meanwhile, a small amount of surfactant benzalkonium chloride was added to make a relatively stable and dispersed lubricant additive in pure water. The structural evolution process of Nb_2C nanosheets with different degrees of oxidation and its tribological behavior when used as a water-based lubricant additive were investigated. The results showed that the moderately oxidized Nb_2C nanosheets, which had a $Nb_2C/Nb_2O_5/C$ composite material system, displayed extremely high stability and anti-wear ability when used as a water lubrication additive.

2 Experimental

2.1 Materials

An accordion-like structured powder of Nb_2C was purchased from Beike Nano Materials Technology Co., Ltd., China, and a tetrabutylammonium hydroxide aqueous solution (TBAOH, 50 wt%) was supplied by Energy Chemical Co., Ltd. In addition, benzalkonium chloride (80 wt%) was purchased from Aladdin Bio-Chem Technology Co., Ltd., and ascorbic acid was obtained from Ruji Biotechnology Development Co., Ltd. Other reagents were purchased from Aladdin Industrial Co. and used directly.

2.2 Preparation of Nb_2C nanosheets with different degrees of oxidation

2.2.1 Intercalation thinning of Nb_2C sheets

The accordion-like original Nb_2C powder and deionized water were configured into a 100-mL aqueous solution at a ratio of 1 mg/mL. According to the method of successfully intercalating and

stripping the MXene material V_2C in Ref. [21], we selected TBAOH as the intercalation agent and a 10 mL/50 wt% TBAOH aqueous solution was added. To prevent oxidation, 20 mg of ascorbic acid was added to the solution. At this time, the entire system was in a reducing atmosphere, and the solution was magnetically stirred in an ice water bath for 12 h to make TBAOH play a role as an intercalation agent within a sufficient amount of time. The mixture obtained was first adjusted to pH7 with hydrochloric acid, then centrifuged at 3,000 rpm for 10 min, and the supernatant was discarded. The above operations were repeated twice with deionized water and anhydrous ethanol. Finally, the residual liquid was treated with a freeze-drying method to obtain a powder.

2.2.2 *Structure regulation of Nb_2C nanosheets*

The powder obtained above was divided into three parts: The first part was prepared as a solution directly with deionized water in the proportion of 0.5 mg/mL, and we could then obtain a type of black Nb_2C solution. The second part was also prepared as an aqueous solution in a proportion of 0.5 mg/mL. On this basis, the powder was magnetically stirred in a 60 ℃ water bath for 6 h, and we obtained a clear and transparent yellow moderately oxidized Nb_2C aqueous solution (MO-Nb_2C). In addition, the third part used the same ratio, but the solution was magnetically stirred at room temperature for 7 days to obtain a completely oxidized Nb_2C aqueous solution (CO-Nb_2C). Moreover, a small amount of surfactant (benzalkonium chloride) was added to these aqueous solutions to improve its stability, and the dosage of surfactant was 0.5 mL/100 mL.

2.3 Characterization of physical and chemical properties

A field emission SEM (FEG 250) was used to observe the micromorphology of the Nb_2C samples. The microstructure of MO-Nb_2C was recorded using TEM (Talos F200x), and the thickness of Nb_2C was evaluated using SPM (Dimension 3100). The structural change of Nb_2C was obtained using XRD (D8 Advance, Bruker), and the XRD scans were measured from 5° to 55° during a 34 min period. In addition, Nb_2C nanosheets with different degrees of oxidation were analyzed using a Raman microscope (RENISHAW, Renishaw) with a 532-nm laser to observe the structure and electronic characteristics. XPS (Axis Ultra DLD) was utilized to explore the chemical binding energy and elements of Nb_2C nanosheets with different degrees of oxidation.

2.4 Tribology test and analysis

Nb_2C nanosheets with different degrees of oxidation were configured into three groups of water-based lubricants according to the mass/volume ratios of 1.0, 0.75, 0.5, and 0.25 mg/mL of pure water. Their tribological behaviors at room temperature were studied using a UMT-3 friction testing machine. Commercially available alumina (Al_2O_3) balls with a diameter of 6 mm were slid reciprocally against 316 steel under a point contact load of 5 N. The sliding frequency was 5 Hz, the test time was 30 min, and the length of the friction track was 5 mm. Each test was repeated at least three times under the same condition using the average friction coefficient (COF) to ensure repeatability. At the same time, an α-step IQ surface contour meter (ASTQ) was used to measure the depth of the wear scar. The wear depth after the friction test was characterized using a surface profiler, and the wear rate (W_s) was calculated from the wear depth, which is given by the following:

$$W_s = \frac{V}{F \cdot L} \tag{1}$$

where V is the total friction volume, F is the normal load, and L is the total distance.

Meanwhile, the three-dimensional (3D) morphology of the wear scars on the 316 steel and the wear scar of the alumina (Al_2O_3) ball were examined using a 3D laser scanning confocal microscope (LSCM, Keyence model VK-X200K), and the Raman spectrum was obtained using a Renishaw inVia Reflex excited by a 532 nm laser. The focused ion beam (FIB, Aurigua) was used to cut the 316 steel for taking TEM images to observe the composition of the friction film and the element distribution in the cross-section of the wear scar.

3 Results and discussion

3.1 Structural transformation of Nb_2C nanosheets with different degrees of oxidation

The dispersity of the Nb_2C sheets with different degrees of oxidation in deionized water is shown in Figs. 1(a)–1(c). From the digital photos, it can be seen that the color of the Nb_2C nanosheets with different degrees of oxidation was obviously different. The aqueous solution of Nb_2C was black, the moderately oxidized Nb_2C showed a clear and transparent yellow color, and the color of the completely oxidized Nb_2C was milky white. It is vividly shown in Fig. 1(b) that there was no precipitation for the Nb_2C nanosheets with a relatively low degree of oxidation added benzalkonium chloride at 15 days, indicating that the surfactants could keep them stable for at least 15 days, but the CO-Nb_2C could not remain stable. This phenomenon indicates that the stability of the system decreased in the case of excessive oxidation. However, at 30 days, even in the presence of surfactants, Nb_2C almost completely precipitated, whereas MO-Nb_2C still showed good stability. Meanwhile, it can also be seen in Fig. 1(d) that MO-Nb_2C had the best stability that its absolute zeta potential could reach approximately 50 mV. By contrast, the zeta potential of CO-Nb_2C was low and irregular, which also proved that the stability of CO-Nb_2C was poor. The working life is one of the most important performance indexes of liquid lubricants, and thus the long dispersion time can be considered as the reliability index of oxidized Nb_2C material as an additive of an aqueous solution, which is also an important prerequisite for the long-term operation of water-based lubricants.

The SEM images of the original accordion-like Nb_2C powder are shown in Fig. 1(e), and scanning probe microscope (SPM) images of Nb_2C nanosheets with different oxidation degrees are shown in Figs. 1(f)–1(h). By comparing the images of Nb_2C powder before and after treatment with an intercalation agent (TBAOH), it was observed that the thickness of Nb_2C was indeed reduced. It can be clearly observed in Fig. 1(g) that there were many circular flakes around the lamellar structure material, and in Fig. 1(h), there were only a few white nanoparticles left. The reason for this phenomenon is that with the progress of oxidation, Nb_2C would gradually change into its oxide Nb_2O_5, and Nb_2O_5 fell off from the original Nb_2C, resulting in white nanoparticles, and when the oxidation degree was too high, the lamellar structure of Nb_2C would gradually disappear, and only the oxidation products Nb_2O_5 were left [25].

The microstructure of the MO-Nb_2C was observed using TEM. From the EDS images shown in Figs. 2(a)–2(d), it can be seen that the elements Nb, C, and O were distributed uniformly on the surface of MO-Nb_2C,

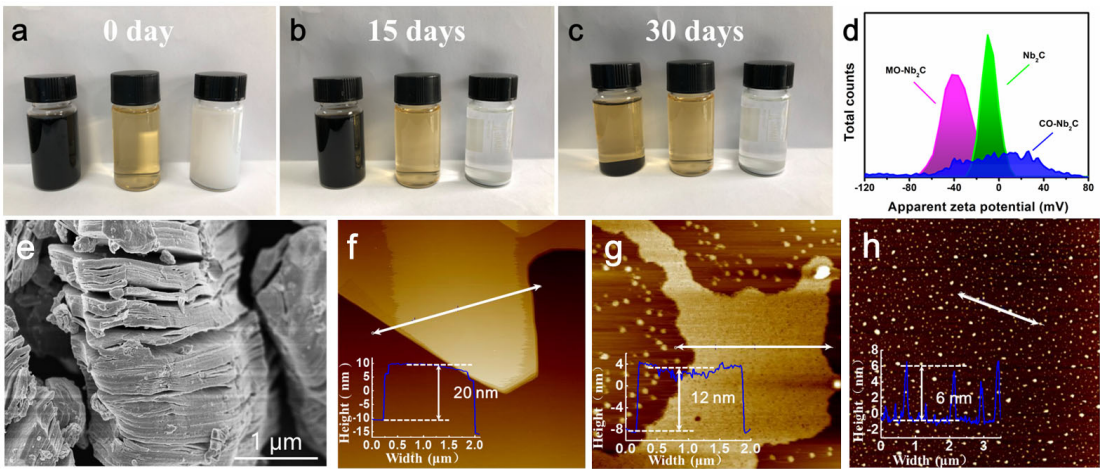

Fig. 1 Digital images of Nb_2C nanosheets with different degrees of oxidation dispersed in water (all concentrations are 0.5 mg/mL) after standing for (a) 0 days, (b) 15 days, and (c) 30 days. (d) Zeta potential of Nb_2C dispersions with different degrees of oxidation. (e) SEM image of the original accordion-like Nb_2C powder. SPM images of (f) Nb_2C nanosheets, (g) MO-Nb_2C, and (h) CO-Nb_2C.

indicating that the oxidation reaction occurred on all parts of the surface. In addition, the HRTEM images of MO-Nb_2C are shown in Figs. 2(e)–2(f). It is worth noting that there were only a few lattice fringes in MO-Nb_2C, and the electron diffraction image also showed that MO-Nb_2C was an amorphous or polycrystalline structure, which was caused by the transformation of Nb_2C into Nb_2O_5 owing to the proceedings of the oxidation, and Nb_2O_5 would fall off from the original structure [26]. Thus, the original Nb_2C with a crystalline structure was transformed into amorphous carbon. Meanwhile, as indicated in the HRTEM image in Fig. 2(g), the oxidation phenomenon was consistent with the white circles in the SPM image, from which we can see obvious lattice stripes, which also proved that the thin and round objects were indeed crystalloid Nb_2O_5, which was the oxidation product of Nb_2C. Moreover, the amorphous ring coexisting with bright diffraction spots in the electron diffraction pattern also proved the existence of the structure of $Nb_2C/Nb_2O_5/C$ in MO-Nb_2C.

To study the crystallographic phase and compositional variation of Nb_2C nanosheets before and after oxidation, X-ray diffraction (XRD) was used. As shown in Fig. 3(a), the peak centered at approximately $2\theta = 9.1°$ and 22.6° could be ascribed to the characteristic peaks of Nb_2C (002) and Nb_2O_5 (001), respectively [27], and the appearance of the characteristic peak at 9.1° showed that Nb_2C was well prepared from Nb_2AlC. This indicates that the oxidized product of Nb_2C was Nb_2O_5. Moreover, when the degree of oxidation increased, the characteristic peak strength of Nb_2C decreased significantly and even disappeared for CO-Nb_2C, whereas the characteristic peak strength of Nb_2O_5 increased at the same time, indicating that the formation of a hybrid material containing Nb_2C, Nb_2O_5, and Nb_2C gradually transformed into Nb_2O_5 with an increase in the degree of oxidation. Meanwhile, the strength of the peak centered at approximately $2\theta = 38.9°$ of the parent material Nb_2AlC decreased, and we speculated that when the degree of oxidation increased, the content of Nb_2AlC decreased.

Raman spectroscopy plays an important role in studying the structural transformation of the materials. To more accurately determine the chemical components of Nb_2C, the Raman spectra of Nb_2C with different degrees of oxidation were obtained, as shown in Fig. 3(b). The bands appearing at 233 cm^{-1} (bending modes of Nb–O–Nb linkages) and 688 cm^{-1} (Nb–O stretching mode) were the characteristic bands of Nb_2O_5 [28]. The presence of these two peaks can be seen in all stages of oxidation. This indicates that the oxidation occurred easily when Nb_2C nanosheets

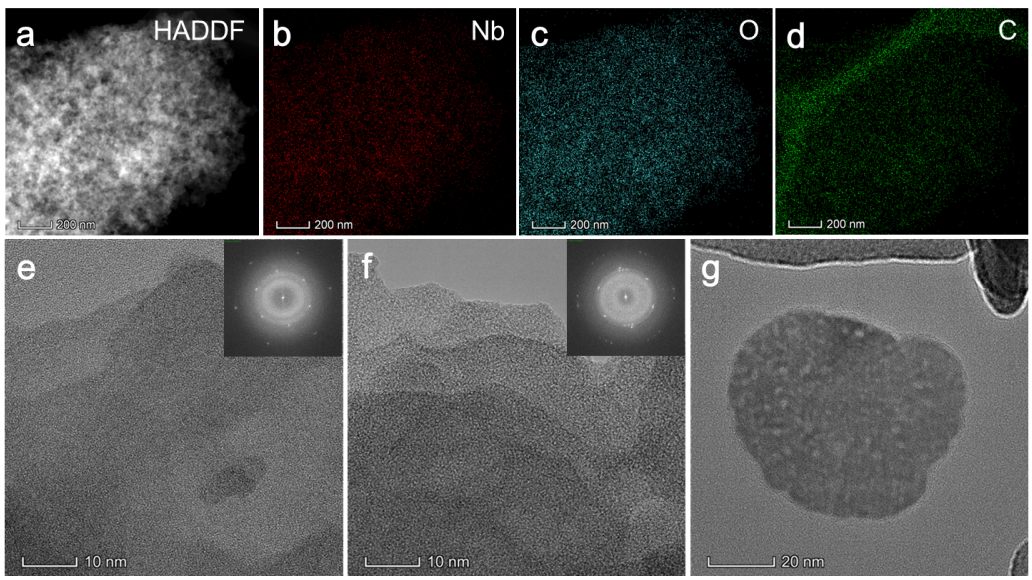

Fig. 2 (a–d) Dark field image and element distribution mapping (Nb, O, C) of MO-Nb_2C and (e–g) HRTEM and SAED images of the edge of MO-Nb_2C.

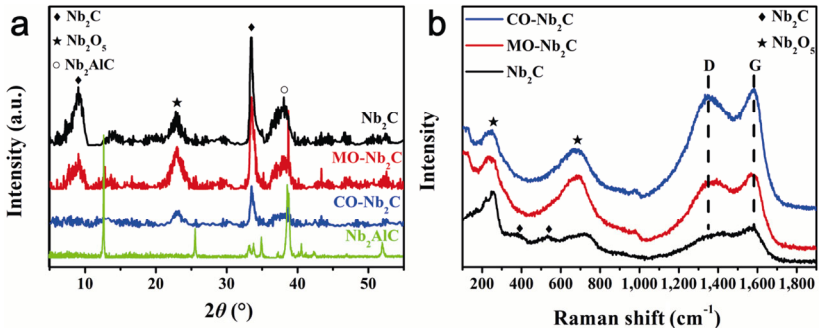

Fig. 3 (a) XRD patterns of Nb_2AlC and Nb_2C and (b) Raman spectra of Nb_2C with different degrees of oxidation.

were thinned, and the strength of the peak at approximately 688 cm^{-1} increased with an increase in the degree of oxidation. Meanwhile, the peaks appearing at 1,381 and 1,589 cm^{-1} were assigned to the D and G bands, respectively. The D band represents the presence of defects in the carbon-based body and the G band is presented owing to the in-plane vibration of sp^2 carbon atoms. This indicates that a hybrid material $Nb_2C/Nb_2O_5/C$ was produced [29, 30].

For the sake of quantitatively analyzing the degree of oxidation Nb_2C, X-ray photoelectron spectroscopy (XPS) was utilized. The X-ray photoelectron spectra of Nb_2C with different degrees of oxidation in the Nb 3d, C 1s, and O 1s regions were fitted by the corresponding components and are shown in Fig. 4. From the Nb 3d spectrum, two strong bands centered at binding energies of approximately 207.8 and 210.7 eV were in good agreement with the binding energy of Nb_2O_5 [31], indicating that oxidation occurred in all sets of samples, which was consistent with the Raman spectra. In addition, some small peaks could be observed in Nb 3d, which can be assigned to Nb^{I}, Nb^{II}, or Nb^{IV} [32], Nb–O [33], and Nb^{3+}–O [34]. The appearance of these peaks also verified the occurrence of the oxidation reaction in Nb_2C. In the C 1s spectrum, a weak band at the binding energy of approximately 282.9 eV can be observed in Nb_2C and MO-Nb_2C, which implies the existence of Nb–C, although it did not appear in the spectrum of CO-Nb_2C [34]. This phenomenon proved that Nb_2C would gradually transform into Nb_2O_5 under excessive oxidation. Further, three main peaks of the C 1s spectrum centered at binding energies of approximately 286.1, 287.1, and 289.2 eV, could be assigned to the C–C bond [35], CH_x, and C–O=O [36], respectively. The main peaks of O 1s corresponded to Nb_2O_5 and C–Nb–OH_x [37]. The distribution of elements Nb, C, and O in Nb_2C with different degrees of oxidation is shown in Table 1. It can be observed that the element content was consistent with the corresponding strength. The Nb/O ratios of Nb_2C, MO-Nb_2C, and CO-Nb_2C were 0.994, 0.311, and 0.216, respectively. These results indicate that MO-Nb_2C was transformed into a hybrid material mainly composed of Nb_2C, Nb_2O_5, and C.

3.2 Tribological behaviors of Nb_2C nanosheets with different degrees of oxidation as water lubricant additive

The tribological behaviors of Nb_2C nanosheets with different degrees of oxidation dispersed in pure water are shown in Fig. 5. To determine the optimal amount of added MXene materials with different degrees of oxidation, we tested an aqueous solution with different Nb_2C mass fractions under the same friction condition (10 N, 2 Hz). Figures 5(a)–5(f) show the COF curves and mean COF of Nb_2C nanosheets with different degrees of oxidation dispersed in pure water with different concentrations. The results showed that the average COF was the lowest when the mass volume ratio of the additive was 0.5 mg/mL for Nb_2C, which was only 0.08. This was 81.2% lower than that of pure water (the average COF of pure water is 0.44). For the MO-Nb_2C, the change in the average COF was in a single trend, and the optimal value of 0.04 was obtained at a concentration of 0.25 mg/mL (the minimum value of the initial experimental group). To explore the optimal solution, we supplemented a set of 0.1 mg/mL data, and the

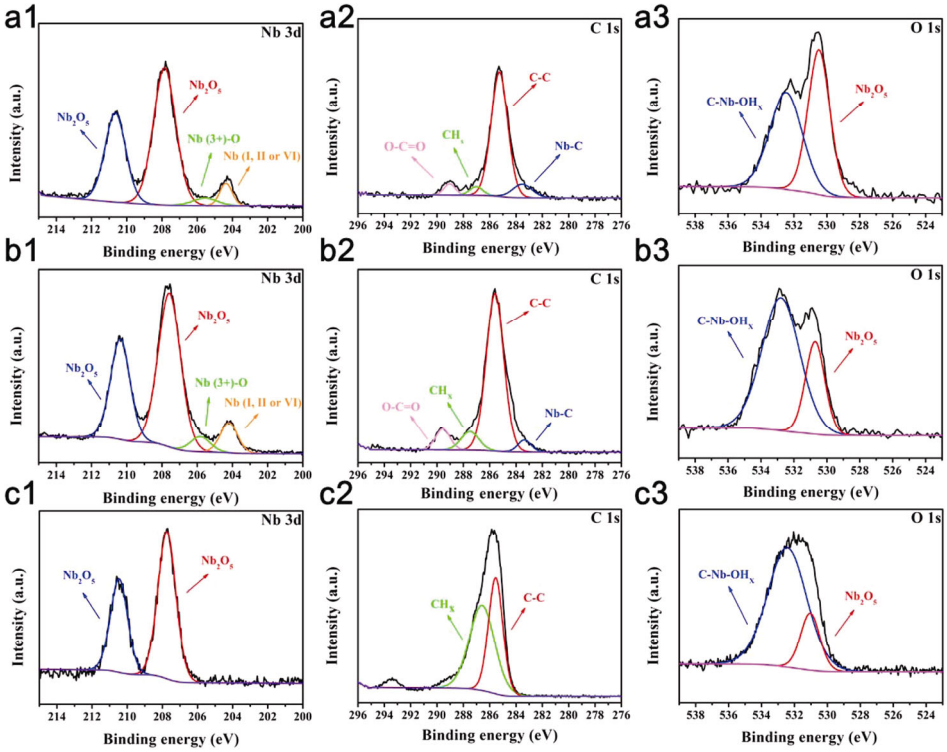

Fig. 4 High-resolution XPS peaks of (a1) Nb 3d, (a2) C 1s, and (a3) O 1s for Nb_2C; (b1) Nb 3d, (b2) C 1s, and (b3) O 1s for MO-Nb_2C; and (c1) Nb 3d, (c2) C 1s, and (c3) O 1s for CO-Nb_2C.

Table 1 Element distribution of Nb and O in Nb_2C powder with different degrees of oxidation.

Sample	Nb (at%)	O (at%)	Nb/O
Nb_2C	26.11	26.28	0.994
MO-Nb_2C	9.38	30.10	0.311
CO-Nb_2C	6.24	28.95	0.216

experimental results showed that the lowest value of COF was indeed obtained at 0.25 mg/mL, which also meant that the average COF of the MO-Nb_2C was 90.3% lower than that of pure water. Moreover, for the CO-Nb_2C sample, the average COF was the lowest when the mass volume ratio of the additive was 0.5 mg/mL, which was 0.12, i.e., 72.7% lower than that of pure water. This means that the Nb_2C material still displayed good tribological properties even in the case of excessive oxidation. The above results showed that, with the addition of Nb_2C nanosheets with different degrees of oxidation, the COF of pure water could be effectively reduced.

As is well known, during the experimental water lubrication process, owing to the load application, the rough summits of the friction pair contact with each other, and a discontinuous fluid film at the microscale will appear in the later period of the friction test, which is called mixed friction or semi-dry friction state. The contact interface contains a solid contact area and a microscale liquid lubrication area. When a fluid film exists, the friction resistance is generally caused by the shear deformation of the rough peak in the solid–solid contact area and the shear action of the fluid in the liquid lubrication area. During the initial stage of the friction test, the friction contact surface gradually changes from a point contact at the microscale to a face contact, which often shows a significant reduction in the COF curve [38]. It can be seen from Figs. 5(a)–5(c) that this phenomenon only occurs in pure water and CO-Nb_2C, which showed that when Nb_2C nanosheets with relatively low oxidation degrees were used as water lubricating additives, the running in the aqueous solution could be effectively improved. Through comparison, it was found that for Nb_2C and MO-Nb_2C, when the friction stage was stable, the average COF also tended to be stable, which showed that the additive had a good dispersion in pure water. The large fluctuation of the COF curve at low concentrations was caused by the lack of

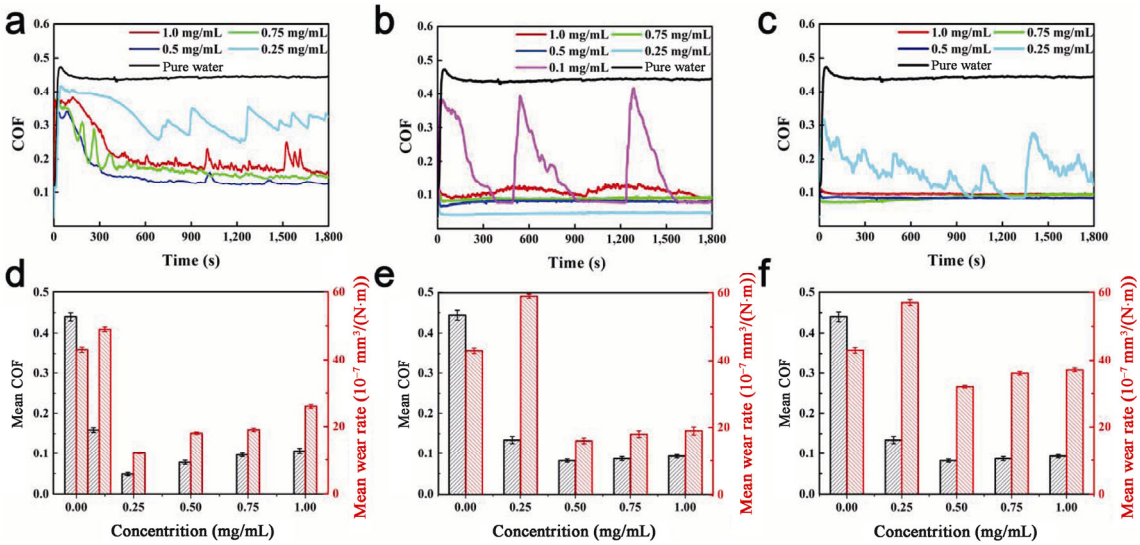

Fig. 5 COF curves, mean COF, and mean wear rate of (a, d) Nb_2C, (b, e) MO–Nb_2C, and (c, f) CO–Nb_2C nanosheets dispersed in pure water with different concentrations.

effective components, which could no longer play the role of effective lubrication. It was found that the overall COF value of CO-Nb_2C was higher than that of Nb_2C and MO-Nb_2C, which was because when the oxidation degree of the system was too high, a large number of Nb_2C nanosheets were transformed into Nb_2O_5 nanoparticles, and the amount of materials that could play the role of an interlayer slip decreased. The mean wear rate and mean COF results of Nb_2C with different degrees of oxidation dispersed in pure water with different concentrations are shown in Figs. 5(d)–5(f). It can be seen that Nb_2C can effectively reduce the wear rate of 316 steel under the water lubrication system, and the wear rate can be reduced up to 62.8% for Nb_2C, 73.1% for MO-Nb_2C, and 25.6% for CO-Nb_2C, respectively. Moreover, the wear rates of the three samples were all higher than those of pure water at low concentrations. This was because at low concentrations, the contents of lamellar Nb_2C and C, which could play an effective lubrication role, were insufficient to support the effective interlayer slip, and the friction film formed was incomplete, which could not provide sufficient lubrication for the friction pair, thus aggravating the wear rate. The above results demonstrated that the MO-Nb_2C showed a better anti-wear property and friction reduction capacity, with an optimal concentration of 0.25 mg/mL.

The 3D morphologies of the wear tracks of MO-Nb_2C with different concentrations were investigated using a laser scanning microscope, as shown in Fig. 6. It could be observed that when the concentration was 0.25 mg/mL, the wear mark size and depth of the MO-Nb_2C were much smaller than those of pure water under the same friction condition. However, at low concentrations, the additive content was insufficient, the formation of friction film at the boundary was discontinuous, and effective lubrication could not be achieved. At the same time, when the concentration was too high, the nanofillers agglomerated, which would promote the wear, and thus it can be seen from the wear scar that the wear degree approached or even exceeded that of pure water.

3.3 Tribological mechanism of Nb_2C nanosheets with different degrees of oxidation

To explore the lubrication mechanism of Nb_2C after oxidation as a water-based lubricant additive with excellent tribological performance, we carried out a series of characterizations on the surface of 316 stainless steel rubbed with a 0.25 mg/mL MO-Nb_2C water solution. The SEM images of the worn scar are shown in Fig. 7(a). When it was rubbed in pure water, there were obvious furrows and cracks on the stainless steel surface, indicating that the wear mode was mainly adhesive wear accompanied by slight abrasive wear. However, the worn scar after

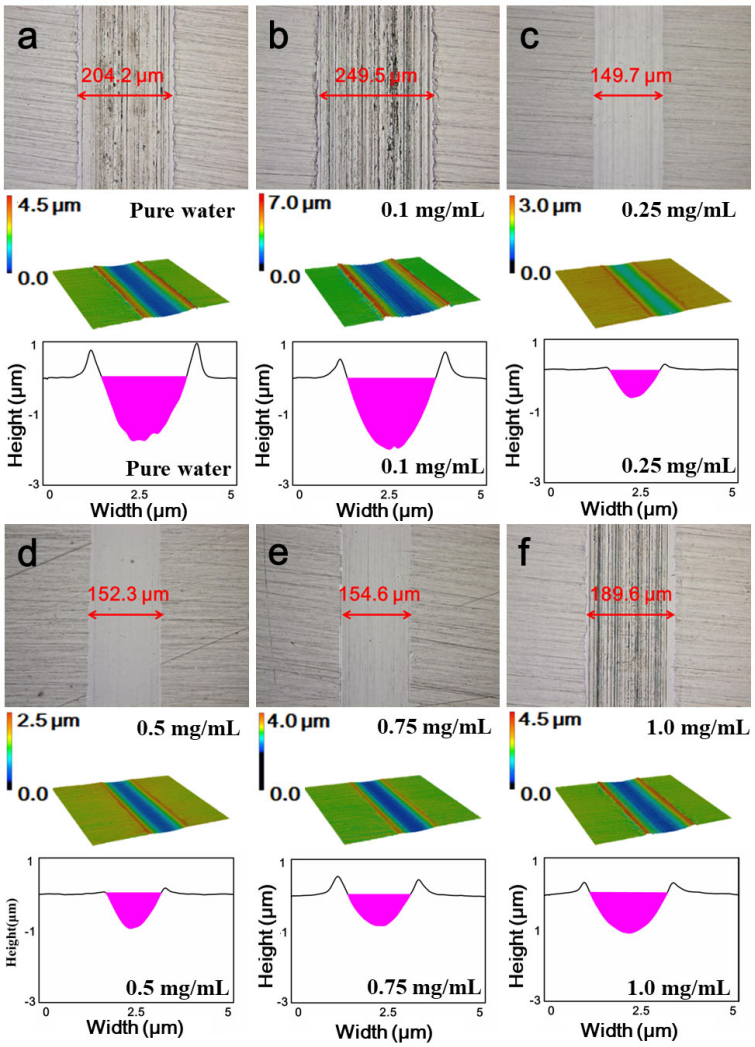

Fig. 6 Micrographs of the wear scars of (a) pure water and MO-Nb_2C nanosheets with concentration of (b) 0.1, (C) 0.25, (d) 0.5, (e) 0.75, and (f) 1.0 mg/mL.

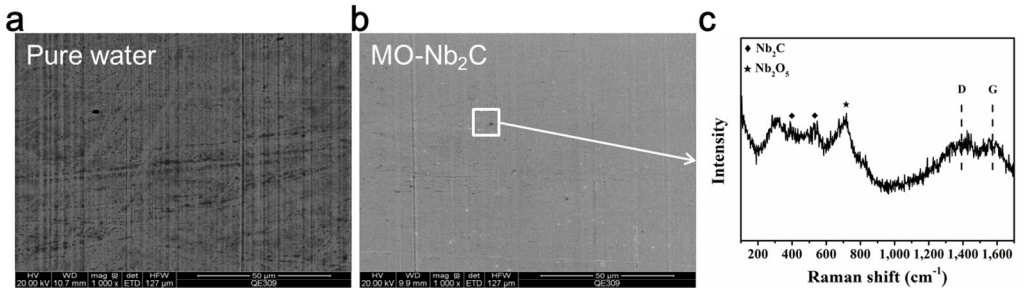

Fig. 7 SEM images of wear scar on the steel disk lubricated by (a) pure water, (b) 0.25 mg/mL MO-Nb_2C water solution, and (c) corresponding Raman spectra of (b).

friction with a 0.25 mg/mL MO-Nb_2C water solution was relatively flat, as shown in Fig. 7(b). Only a few minor furrows were produced during friction, and it was found that there were plenty of small white spots existing among the wear scars. We speculated that this was because the Nb_2O_5 formed by Nb_2C after oxidation filled the wear area, whereas the original lamellar Nb_2C and the C produced by

oxidation were adsorbed on the surface of the friction pair, forming a lubrication protective film. To prove this, we employed the Raman spectrum to test the worn surface of stainless steel lubricated with 0.25 mg/mL MO-Nb_2C. As shown in Fig. 7(c), the typical characteristic peaks of carbon and Nb_2C appeared in the corresponding Raman spectrum, which confirmed that the original lamellar Nb_2C and C formed in the oxidation of Nb_2C deposited on the worn surface to form a protective lubricating film. The high strength characteristic peak at 688 cm^{-1} also indicated that Nb_2O_5 was abundant in the wear scar.

At the same time, to analyze the lubrication mechanism of samples from a more microscopic perspective, we conducted a TEM test on the cross-section of the wear scars lubricated by an aqueous solution of MO-Nb_2C. As shown in Figs. 8(a)–8(c), the average thickness of the friction film formed in the cross-section of the worn scar of MO-Nb_2C was approximately 75 nm, which was much thicker than the other two samples. In the area with serious wear, the thickness could reach more than 200 nm, indicating that the MO-Nb_2C nanosheets showed a strong wear repairability, and it also proved that the structure of $Nb_2C/Nb_2O_5/C$ was better than that of a single Nb_2C or excessive oxidized Nb_2C. Moreover, to explore the chemical composition of the worn surface filled with MO-Nb_2C nanosheets and reveal its lubrication mechanism, an element distribution mapping test was employed. It can clearly be seen that Nb and O existed on the friction film, indicating that Nb_2O_5 can enter and fill the worn area well and C can also be found in the surface area of the wear scar, meaning the formation of a carbon-based lubricating protective film, which was consistent with the image of the Raman spectra.

Based on the above results, we proposed the tribological mechanism of MO–Nb_2C nanosheets as a water-based lubricant additive with excellent

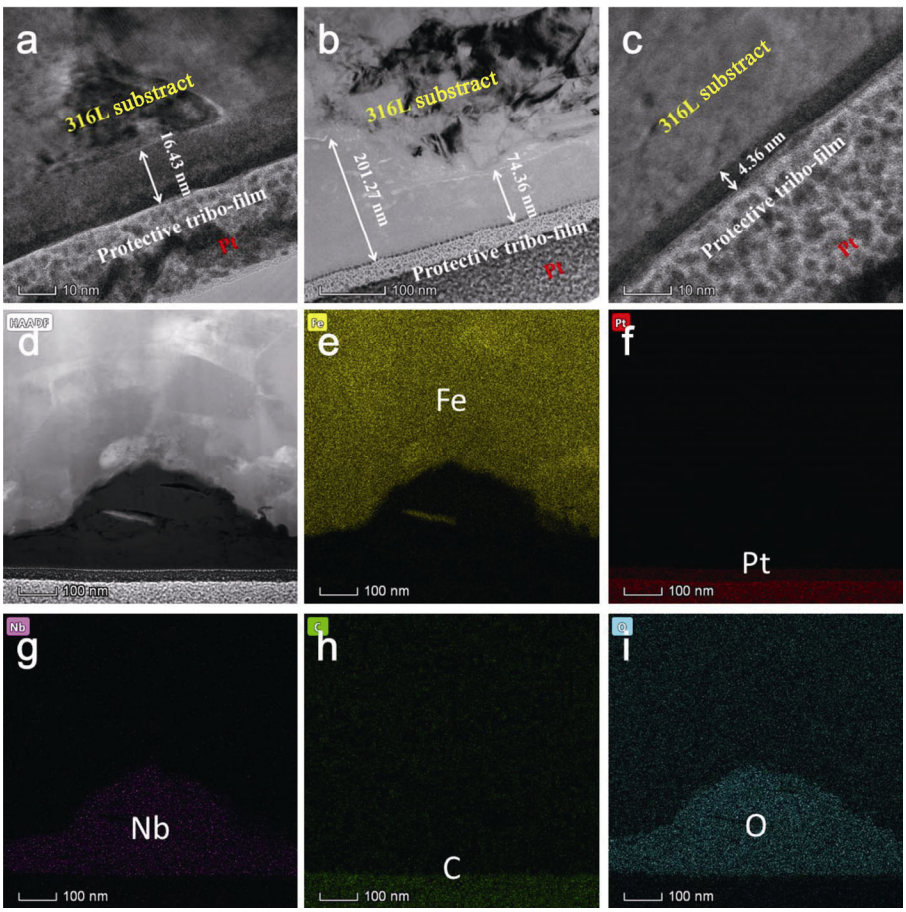

Fig. 8 TEM images of the cross-section of wear scar lubricated using (a) Nb_2C, (b) MO-Nb_2C, and (c) CO-Nb_2C; (d–i) element distribution mapping of the cross-section of wear scar lubricated using MO-Nb_2C nanosheet enhanced water solution.

lubrication performance. During the recent oxidation treatment, the original Nb_2C was transformed into the $Nb_2C/Nb_2O_5/C$ composite structure. Among them, layered C and Nb_2C entered between the friction pair and adsorbed on the surface of the friction pair to form a lubrication protection film to prevent the friction pair from direct contact. The improvement of the tribological property of MO-Nb_2C was due to the synergistic effect of Nb_2C and C, rather than the contribution of pure C or Nb_2C, which is a key point that resulted in the different friction properties of Nb_2C, MO-Nb_2C, and CO-Nb_2C. At the same time, the oxidation product Nb_2O_5, with its small size, could enter and fill in the worn area, reducing the wear rate. Their synergistic effect endowed the MO-Nb_2C with excellent tribological performance.

In addition, some illustrations of the excellent tribological properties of black phosphorus (BP) with the same 2D layered structure, as determined by previous researchers, also significantly aided this study [39–42]. The interaction between the nanoparticles and water contributed to the lubrication. The water layer retained by BP–OH nanosheets could provide an extremely low shear resistance, and the ambient degradation of BP also showed a positive effect. All of the above contents provide a novel way to explain the phenomenon in which Nb_2C nanosheets with different degrees of oxidation all showed good tribological performances, and we will focus on these aspects in our future studies.

4 Conclusions

In this study, we added an intercalation agent (TBAOH) to an accordion-like Nb_2C powder, with only a simple treatment, and obtained Nb_2C nanosheets. At the same time, we prepared Nb_2C with different degrees of oxidation, and prepared a long-term stable aqueous solution. On this basis, friction tests of Nb_2C samples with different degrees of oxidation were carried out, and the results showed that the moderately oxidized Nb_2C water solution displayed excellent tribological performances, with the COF decreasing by 90.3% and the wear rate decreasing by 73.1% compared with pure water. As the oxidation proceeded, the original Nb_2C gradually changed into a structure of $Nb_2C/Nb_2O_5/C$. The Nb_2O_5 nanoparticles filled in the worn zone and the layered Nb_2C and C adsorbed on the surface of the friction pair to form a lubricating film, and their combined action resulted in excellent lubrication. Meanwhile, we found that the lubrication property of Nb_2C was always better than that of pure water, regardless of its degree of oxidation. Based on these conclusions, an excellent friction reduction and wear resistance of moderately oxidized Nb_2C display significant potential as a nanoadditive in the application of water lubrication technology.

Acknowledgements

We would like to express our thanks to the National Natural Science Foundation of China (51775540), Zhejiang Provincial Natural Science Foundation of China (LR21E050001), and the Youth Innovation Promotion Association, CAS (2017338).

References

[1] Liu J, Qi Y Z, Li Q Y, Duan T Y, Yue W, Vadakkepatt A, Ye C, Dong Y L. Vacancy-controlled friction on 2D materials: Roughness, flexibility, and chemical reactions. *Carbon* **142**: 363–372 (2019)

[2] Wang H D, Liu Y H, Liu W R, Wang R, Wen J G, Sheng

H P, Peng J F, Erdemir A, Luo J B. Tribological behavior of NiAl-layered double hydroxide nanoplatelets as oil-based lubricant additives. *ACS Appl Mater Interfaces* **9**(36): 30891–30899 (2017)

[3] Mai Y J, Chen F X, Lian W Q, Zhang L Y, Liu C S, Jie X H. Preparation and tribological behavior of copper matrix composites reinforced with nickel nanoparticles anchored graphene nanosheets. *J Alloys Compd* **756**: 1–7 (2018)

[4] Naguib M, Mochalin V N, Barsoum M W, Gogotsi Y. 25th anniversary article: MXenes new family of two-dimensional materials. *Adv Mater* **26**(7): 992–1005 (2014)

[5] Wu H, Zhao J W, Xia W Z, Cheng X W, He A S, Yun J H, Wang L Z, Huang H, Jiao S H, Huang L, *et al*. A study of the tribological behaviour of TiO_2 nano-additive water-based lubricants. *Tribol Int* **109**: 398–408 (2017)

[6] Yan S, Lin B, Liu F, Yan F G. Friction and wear of self-mated SiC and Si_3N_4 in green water-based lubricant. *Int J Precis Eng Manuf* **13**(7): 1067–1072 (2012)

[7] Hu Y W, Wang Y X, Zeng Z X, Zhao H C, Ge X W, Wang K, Wang L P, Xue Q J. PEGlated graphene as nanoadditive for enhancing the tribological properties of water-based lubricants. *Carbon* **137**: 41–48 (2018)

[8] Liang S S, Shen Z G, Yi M, Liu L, Zhang X J, Ma S L. *In-situ* exfoliated graphene for high-performance water-based lubricants. *Carbon* **96**: 1181–1190 (2016)

[9] Song H J, Li N. Frictional behavior of oxide graphene nanosheets as water-base lubricant additive. *Appl Phys A* **105**(4): 827–832 (2011)

[10] Feng X F, Kwon S, Park J Y, Salmeron M. Superlubric sliding of graphene nanoflakes on graphene. *ACS Nano* **7**(2): 1718–1724 (2013)

[11] Lee H, Lee N, Seo Y, Eom J, Lee S. Comparison of frictional forces on graphene and graphite. *Nanotechnology* **20**(32): 325701 (2009)

[12] Marchetto D, Feser T, Dienwiebel M. Microscale study of frictional properties of graphene in ultra high vacuum. *Friction* **3**(2): 161–169 (2015)

[13] Kinoshita H, Nishina Y, Alias A A, Fujii M. Tribological properties of monolayer graphene oxide sheets as water-based lubricant additives. *Carbon* **66**: 720–723 (2014)

[14] Liu Y H, Wang X K, Pan G S, Luo J B. A comparative study between graphene oxide and diamond nanoparticles as water-based lubricating additives. *Sci China Technol Sci* **56**(1): 152–157 (2013)

[15] Ci X J, Zhao W J, Luo J, Wu Y M, Ge T H, Xue Q J, Gao X L, Fang Z W. How the fluorographene replaced graphene as nanoadditive for improving tribological performances of GTL-8 based lubricant oil. *Friction*, in press, DOI 10.1007/s40544-019-0350-y.

[16] Wang W, Xie G X, Luo J B. Black phosphorus as a new lubricant. *Friction* **6**(1): 116–142 (2018)

[17] Naguib M, Mashtalir O, Carle J, Presser V, Lu J, Hultman L, Gogotsi Y, Barsoum M W. Two-dimensional transition metal carbides. *ACS Nano* **6**(2): 1322–1331 (2012)

[18] Li M, Lu J, Luo K, Li Y B, Chang K K, Chen K, Zhou J, Rosen J, Hultman L, Eklund P, *et al*. Element replacement approach by reaction with lewis acidic molten salts to synthesize nanolaminated MAX phases and MXenes. *J Am Chem Soc* **141**(11): 4730–4737 (2019)

[19] Zhou J, Zha X H, Zhou X B, Chen F Y, Gao G L, Wang S W, Shen C, Chen T, Zhi C Y, Eklund P, *et al*. Synthesis and electrochemical properties of two-dimensional hafnium carbide. *ACS Nano* **11**(4): 3841–3850 (2017)

[20] Tang X, Guo X, Wu W J, Wang G X. 2D metal carbides and nitrides (MXenes) as high-performance electrode materials for lithium-based batteries. *Adv Energy Mater* **8**(33): 1801897 (2018)

[21] Maleski K, Mochalin V N, Gogotsi Y. Dispersions of two-dimensional titanium carbide MXene in organic solvents. *Chem Mater* **29**(4): 1632–1640 (2017)

[22] Zheng J S, Diao J L, Jin Y Z, Ding A L, Wang B, Wu L Z, Weng B, Chen J C. An inkjet printed Ti_3C_2–GO electrode for the electrochemical sensing of hydrogen peroxide. *J Electrochem Soc* **165**(5): B227–B231 (2018)

[23] Naguib M, Unocic R R, Armstrong B L, Nanda J. Large-scale delamination of multi-layers transition metal carbides and carbonitrides "MXenes". *Dalton Trans* **44**(20): 9353–9358 (2015)

[24] Natu V, Hart J L, Sokol M, Chiang H, Taheri M L, Barsoum M W. Edge capping of 2D-MXene sheets with polyanionic salts to mitigate oxidation in aqueous colloidal suspensions. *Angew Chem* **131**(36): 12785–12790 (2019)

[25] Su T M, Peng R, Hood Z D, Naguib M, Ivanov I N, Keum J K, Qin Z Z, Guo Z H, Wu Z L. One-step synthesis of Nb_2O_5/C/Nb_2C (MXene) composites and their use as photocatalysts for hydrogen evolution. *ChemSusChem* **11**(4): 688–699 (2018)

[26] Naguib M, Mashtalir O, Lukatskaya M R, Dyatkin B, Zhang C F, Presser V, Gogotsi Y, Barsoum M W. One-step synthesis of nanocrystalline transition metal oxides on thin sheets of disordered graphitic carbon by oxidation of MXenes. *Chem Commun* **50**(56): 7420–7423 (2014)

[27] Naguib M, Halim J, Lu J, Cook K M, Hultman L, Gogotsi Y, Barsoum M W. New two-dimensional niobium and vanadium carbides as promising materials for Li-ion batteries. *J Am Chem Soc* **135**(43): 15966–15969 (2013)

[28] Peng C, Wei P, Chen X, Zhang Y L, Zhu F, Cao Y H,

Wang H J, Yu H, Peng F. A hydrothermal etching route to synthesis of 2D MXene (Ti_3C_2, Nb_2C): Enhanced exfoliation and improved adsorption performance. *Ceram Int* **44**(15): 18886–18893 (2018)

[29] Kudin K N, Ozbas B, Schniepp H C, Prud'Homme R K, Aksay I A, Car R. Raman spectra of graphite oxide and functionalized graphene sheets. *Nano Lett* **8**(1): 36–41 (2008)

[30] Ci X J, Zhao W J, Luo J, Wu Y M, Ge T H, Shen L, Gao X L, Fang Z W. Revealing the lubrication mechanism of fluorographene nanosheets enhanced GTL-8 based nanolubricant oil. *Tribol Int* **138**: 174–183 (2019)

[31] Qamar M, Abdalwadoud M, Ahmed M I, Azad A M, Merzougui B, Bukola S, Yamani Z H, Siddiqui M N. Single-pot synthesis of ⟨001⟩-faceted N-doped Nb_2O_5/reduced graphene oxide nanocomposite for efficient photoelectrochemical water splitting. *ACS Appl Mater Interfaces* **7**(32): 17954−17962 (2015)

[32] Marques M T, Ferraria A M, Correia J B, Rego A M B D, Vilar R. XRD, XPS and SEM characterisation of Cu–NbC nanocomposite produced by mechanical alloying. *Mater Chem Phys* **109**(1): 174–180 (2008)

[33] Zhang W B, Wu W D, Wang X M, Cheng X L, Yan D W, Shen C L, Peng L P, Wang Y Y, Bai L. The investigation of NbO_2 and Nb_2O_5 electronic structure by XPS, UPS and first principles methods. *Surf Interface Anal* **45**(8): 1206–1210 (2013)

[34] Halim J, Cook K M, Naguib M, Eklund P, Gogotsi Y, Rosen J, Barsoum M W. X-ray photoelectron spectroscopy of select multi-layered transition metal carbides (MXenes). *Appl Surf Sci* **362**: 406–417 (2016)

[35] Yue X Z, Yi S S, Wang R W, Zhang Z T, Qiu S L. Cadmium sulfide and nickel synergetic Co-catalysts supported on graphitic carbon nitride for visible-light-driven photocatalytic hydrogen evolution. *Sci Rep* **6**: 22268 (2016)

[36] Jayaweera P M, Quah E L, Idriss H. Photoreaction of ethanol on TiO_2(110) single-crystal surface. *J Phys Chem C* **111**(4): 1764–1769 (2007)

[37] Zhang C J, Kim S J, Ghidiu M, Zhao M Q, Barsoum M W, Nicolosi V, Gogotsi Y. Layered orthorhombic Nb_2O_5@$Nb_4C_3T_x$ and TiO_2@$Ti_3C_2T_x$ hierarchical composites for high performance Li-ion batteries. *Adv Funct Mater* **26**(23): 4143–4151 (2016)

[38] Elomaa O, Singh V K, Iyer A, Hakala T J, Koskinen J. Graphene oxide in water lubrication on diamond-like carbon vs. stainless steel high-load contacts. *Diam Relat Mater* **52**: 43–48 (2015)

[39] Ren X Y, Yang X, Xie G X, Luo J B. Black phosphorus quantum dots in aqueous ethylene glycol for macroscale superlubricity. *ACS Appl Nano Mater* **3**(5): 4799–4809 (2020)

[40] Wang W, Xie G X, Luo J B. Superlubricity of black phosphorus as lubricant additive. *ACS Appl Mater Interfaces* **10**(49): 43203–43210 (2018)

[41] Wu S, He F, Xie G X, Bian Z L, Ren Y L, Liu X Y, Yang H J, Guo D, Zhang L, Wen S Z, *et al*. Super-slippery degraded black phosphorus/silicon dioxide interface. *ACS Appl Mater Interfaces* **12**(6): 7717–7726 (2020)

[42] Wu S, He F, Xie G X, Bian Z L, Luo J B, Wen S Z. Black phosphorus: Degradation favors lubrication. *Nano Lett* **18**(9): 5618–5627 (2018)

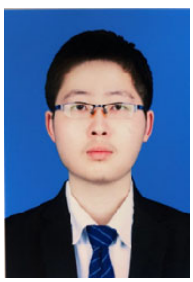

Hao CHENG. He received his bachelor degree in material science and engineering in 2018 from Nanjing Institute of Technology, Nanjing, China. He is now a master student at Ningbo Institute of Materials Technology and Engineering, Chinese Academy of Sciences (CAS), China. His research interests include 2D-materials and lubrication.

Wenjie ZHAO. He received his Ph.D. degree in materials science from Lanzhou Institute of Chemical Physics, CAS, in 2010. Then, he joined the Key Laboratory of Marine Materials and Related Technologies at Ningbo Institute of Materials Technology and Engineering, CAS. His current position is a professor. His research areas cover the tribology of composite materials, 2D nanomaterials preparation, interfacial physical chemistry, and protective coatings.